forests

MDPI

Article

Factors Influencing the Geographical Distribution of *Dendroctonus armandi* (Coleoptera: Curculionidae: Scolytidae) in China

Hang Ning [1], Lulu Dai [1], Danyang Fu [1], Bin Liu [1], Honglin Wang [1] and Hui Chen [1,2,*]

[1] College of Forestry, Northwest A&F University, Yangling 712100, Shaanxi, China; ninghang92@gmail.com (H.N.); dailulu015@163.com (L.D.); fudanyang@nwsuaf.edu.cn (D.F.); lb1006330993@163.com (B.L.); wlindking@hotmail.com (H.W.)

[2] State Key Laboratory for Conservation and Utilization of Subtropical Agro-Bioresources (South China Agricultural University), Guangdong Key Laboratory for Innovative Development and Utilization of Forest Plant Germplasm, College of Forestry and Landscape Architecture, South China Agricultural University, Guangzhou 510642, China

* Correspondence: chenghui@nwsuaf.edu.cn; Tel./Fax: +86-029-87082083

Received: 7 April 2019; Accepted: 12 May 2019; Published: 16 May 2019

Abstract: In order to prevent any further spread of *Dendroctonus armandi* (Coleoptera: Curculionidae: Scolytidae), it is important to clarify its geographic distribution in China. Species Distribution Models were used to identify the variables influencing the distribution of *D. armandi* in China, and to create maps of its distribution. *D. armandi* almost exclusively attacked *Pinus armandi* Franch (IP (frequency of its incidence) = 98.2%), and its distribution is focused on the Qinling Mountains and the Ta-pa Mountains. The current distribution of *P. armandi* does not limit the distribution of *D. armandi*, despite the host occurring in in northern and southwestern China. Temperature and precipitation limit the current distribution of this beetle. The mean temperature of coldest quarter (−5 °C) does not guarantee that *D. armandi* larvae can overwinter in northern China, and the precipitation of wettest quarter plays an important role in the dispersal and colonization of *D. armandi* adults in southwestern China. Therefore, the ecological niche of this beetle is relatively narrow when it comes to these environmental variables. The climatic conditions where this beetle inhabit are different from the prevalent climate in the Qinling Mountains and the Ta-pa Mountains. At the meso- and micro-scale levels, terrain variables create habitat selection preferences for *D. armandi*. *D. armandi* predominately colonizes trees on the southern slopes of valleys and canyons with elevations between 1300 m a.s.l and 2400 m a.s.l.

Keywords: *Dendroctonus armandi*; species distribution models; limiting factors; potential distribution

1. Introduction

Geographic distribution is of great importance in the study of population dynamics, which involve exogenous and endogenous factors [1,2]. Together, these factors constitute the population ecology processes, which limits the abundance and geographic distribution of species [3–5]. Generally, the studies of species distribution only used basic information from museums, scientific collections, and related literatures [6,7]. Combining this basic information with additional data on climate, biology, and topography is important in fully understanding the geographic distributions of species [8,9].

Species distribution models (SDMs) have been widely used in the prediction of species distribution. An increasing availability of spatial data, as well as high resolution bioclimatic data, have continuously enhanced the prerequisites that are needed for successful SDMs and the assessment of factors affecting the magnitude and extent of a potential invasion [10]. Furthermore, SDMs have evolved along with the

increasing variety and availability of the statistical methods, digital biological, and environmental data with which they are built in a geographic information system [11]. SDMs has the strong advantage of improving the utility and reliability in the analysis of the potential distribution of species with a relatively broad range distribution and little knowledge of biology and ecology [12,13]. Besides, SDMs have become an important and widely used decision-making tool for a variety of biogeographical applications, such as studying the effects of climate change, identifying potential protected areas, determining the locations that are potentially susceptible to invasion, and mapping vector-borne disease spread and risk [14]. SDMs, including Bioclimatic analysis (BIOCLIM), Genetic Algorithm for Rule-set Prediction (GARP), Ecological Niche Factor Analysis (ENFA), Maximum Entropy (MaxEnt), and CLIMEX [15–17], have been widely used in many different applications. Srivastava et al. (2018) [10] used Ensemble modelling, which includes BIOCLIM, GARP, and MaxEnt to map the potential distribution of the *Yushania maling* (Gamble) in the Darjeeling Himalayas. Giusti et al. (2017) [16] employed ENFA to characterize ecological niche and map the potential distribution of *Viminella flagellum* (Alcyonacea: Ellisellidae) in southeastern Sardinian waters. Van Gils et al. (2014) [18] applied MaxEnt to predict the year-round and seasonal bear distribution in Majella National Park, Italy. Huang et al. (2019) [19] used the CLIMEX to predict the current and future potential distributions of the *Eucalyptus* pest *Leptocybe invasa* (Hymenoptera: Eulophidae) in China. While integrating the diverse data on biology, climate, and topography, SDMs has developed the more credible potential distribution and species responses to past and future climatic conditions [8].

Dendroctonus armandi Tsai and Li (Coleoptera: Curculionidae: Scolytidae) is a cryptic herbivore that completes its life cycle under the bark of the conifer, except during a brief dispersal period, when the adults search for new host trees. Voltinism varies with elevation in the Qinling Mountains. Typically, there are two generations per year at elevations lower than 1700 m a.s.l, three generations within two years between 1700 and 2150 m a.s.l., and one generation per year above 2150 m a.s.l. As a pioneer species, it unites blue-stain fungus *Leptographium qinlingensis* to invade healthy *Pinus armandi* Franch more than 30 years and triggers the secondary bark beetles to attack the infected or withered host trees [20]. Females are always the first to bore through the bark of the host and then attract males with aggregation pheromones for colonization and reproduction [21]. Outbreaks of this bark beetle have constantly occurred over the past 30 years in the Qinling Mountains and the Ta-pa Mountains, where the zone has distinctive geomorphic and geologic or tectonic features to differentiate it from neighboring zones, which causes landscape-level mortality to the healthy *P. armandi*, a native conifer that is primarily distributed along the Qinling Mountains and Ta-pa Mountains [22]. *P. armandi* plays an important ecological role by reducing soil erosion and it is an important element of regional socioeconomic development. The Qinling Mountains gradually decline from west to east, which is the most important north-south boundary line in China's geography. The rivers that run through the mountains are mostly cross-cutting or oblique, which result in many canyons with steep terrain in the upper and middle reaches of the rivers. The Ta-pa Mountains range from northwest to southeast. They also have many valleys and steep canyons that were cut by a river [23].

Although *Dendroctonus armandi* (Coleoptera: Curculionidae: Scolytidae) is significant as a forest pest, its biology, ecology, and geographic distribution are relatively poorly understood. As such, a detailed knowledge regarding the population distribution of *D. aramndi* is required for pest management. SDMs have also been widely applied to the potential management of bark beetles. For example, Duque-Lazo et al. (2017) [24] used the Andalusian forest health monitoring network (SEDA Network) to assess the current distribution of the xylophage beetles, while using the Kernel Density Estimation approach, and the current and future distributions using ensemble SDMs. Buse et al. (2007) [25] used species distribution modelling based on datasets from Central Europe to understand the species–habitat relationships and find the environmental variables that are responsible for habitat selection of the longhorn beetle *Cerambyx cerdo* L. (Coleoptera, Cerambycidae). Lausch et al. (2011) [26] used ENFA to quantitatively analyse the factors affecting the spatio-temporal dispersion of *Ips typographus* (L.) in Bavarian Forest National Park. In this study, we used BIOCLIM, ENFA, and

MaxEnt to model the potential distribution of *D. armandi* in China. We aimed to use SDMs to analyze the main factors influencing the distribution of *D. armandi*, and ultimately provide critical information to cope with the further range expansion of *D. armandi*.

2. Materials and Methods

2.1. Study Area

We used a proxy study area that covered the natural distribution of *P. armandi*, which was located between 24° N and 36° N and between 98° E and 111° E, and it included multiple climate type zones (Figure 1). In order to better understand the climatic environment of *D. armandi*, the distribution profile of the host is as follows (Table 1) [27,28].

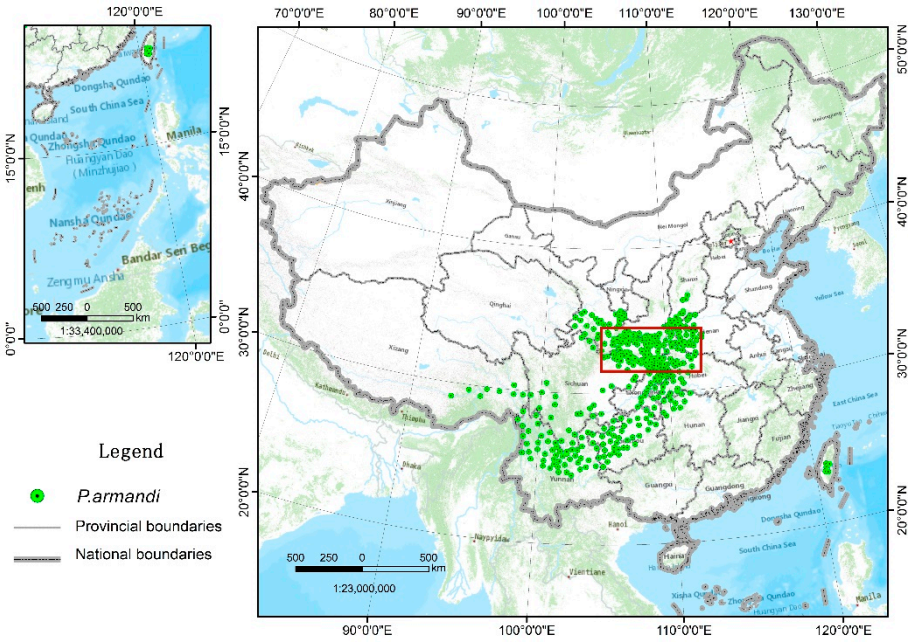

Figure 1. Present distribution of *Pinus armandi* Franch in China. The area where *Dendroctonus armandi* (Coleoptera: Curculionidae: Scolytidae) is located in the red box.

Table 1. Profile of the natural distribution of *Pinus armandi* Franch.

Climate Type	Longitude/Latitude	Environmental Overview	Distribution Range
North subtropical evergreen deciduous broad-leaved mixed forest belt	29° N–33° N 105° E–111° E	The annual average temperature is 7–16 °C, the extreme minimum temperature is −5 to −22 °C, the extreme maximum temperature is 29–41 °C, the accumulated temperature of ≥10 °C is 2300–4500 °C, the annual precipitation is 1000–1400 mm.	The junction of Shannxi, Sichuan, Gansu, Hubei, Chongqing and Henan provinces in southern the Qinling Mountains, including Ta-ba Mountains, Micang Mountains and Wushan Mountains.
Central subtropical evergreen broad-leaved forest belt	24° N–29° N 98° E–105° E	The annual average temperature is 10.5–18.3 °C, the extreme minimum temperature is −1.7 to −13.8 °C, the extreme maximum temperature is 33.8 °C, the accumulated temperature of ≥10 °C is 4500 to 5500 °C, the annual precipitation is 500–1400 mm.	Northeast and Northwest Yunnan, western Guizhou, and southwestern Sichuan.
Warm temperate deciduous broad-leaved forest belt	33° N–36° N 105° E–113° E	The annual average temperature is 6–13 °C, the extreme minimum temperature is −18 to −24 °C, the extreme maximum temperature is 30–38 °C, the accumulated temperature of ≥10 °C is 2000–4000 °C, the annual precipitation is 70–1000 mm.	All the distribution in northern the Qinling Mountains, include the southern the Zhongtiao Mountains in Shanxi, the Liupan Mountains in Ningxia, the Longshan in Gansu, the Funiu Mountains in Henan.

2.2. Data

2.2.1. Ecogeographical Variables Layers

We used ecogeographical variables layers as the main input to create the potential distribution of *D. armandi* according to its bioclimatic requirements [29]. Bioclimatic variables were downloaded from the WorldClim open climate data for SDMs and Arc-GIS v.10.2 (Environmental System Research Institute Inc., Redlands, CA, USA) [30]. WorldClim is a set of global climate layers (gridded climate data) with a spatial resolution of 5-arc min., which is available at www.worldclim.org, including 19 default bioclimatic variables. Terrain layers were freely downloaded from edcdaac.usgs.gov/gtopo30/gtopo30.html, which is a digital elevation model for the world, as developed by United States Geological Survey (USGS). It is split into 33 tiles that were stored in the USGS digital elevation model (DEM) file format. The layers contain a number of raster grids, each of which variable layer must all have the same geographic bounds and cell size.

To reduce the multi-collinearity among the 19 bioclimatic variables, we used MaxEnt v.3.3.1 (www.cs.princeton.edu/~{}schapire/maxent) to select significant factors according to their level of contribution [31]. Variables with higher maximum entropy gains were retained. Examining multi-collinearity carried out further exclusion of the variables, and highly correlated variables ($r \geq 0.85$ Pearson correlation coefficient) were eliminated [32]. The results of the reduction of bioclimatic variables are as follows (Table 2). In addition, principal component analysis (PCA) is also used as a complement to variables selection. This result can be found in Table 3.

Table 2. Contribution of each of 8 selected variables in MaxEnt for *D. armandi*.

Code	Bioclimatic Variables	% Contribution
Bio11	Mean temp of coldest quarter (°C)	25.6
Bio9	Mean temp of driest quarter (°C)	15.3
Bio6	Minimum temp of coldest month (°C)	14.1
Bio1	Annual mean temp (°C)	11.5
Bio16	Precipitation of wettest quarter (mm)	10.8
Bio18	Precipitation of warmest quarter (mm)	9.7
Bio13	Precipitation of wettest month (mm)	8.6
Bio12	Annual precipitation (mm)	4.5

Table 3. Principal component analysis (PCA) of Bioclim climatic variables in relation to the occurrence of *D. armandi*.

Title 1	Climatic Variables	Eigenvalues		
		Component 1	Component 2	Component 3
Bio1 [a]	Annual mean temp (°C)	0.70	0.71	−0.05
Bio2 [a]	Mean diurnal range (°C)	−0.58	0.42	0.56
Bio3	Isothermality	−0.62	−0.19	0.25
Bio4	Temperature seasonality	−0.16	0.76	0.51
Bio5	Maximum temp of warmest month (°C)	0.51	0.83	0.20
Bio6 [a]	Minimum temp of coldest month (°C)	0.84	0.40	−0.30
Bio7	Temperature annual range	−0.34	0.67	0.61
Bio8	Mean temp of wettest quarter (°C)	0.63	0.77	0.05
Bio9 [a]	Mean temp of driest quarter (°C)	0.78	0.54	−0.22
Bio10	Mean temp of warmest quarter (°C)	0.59	0.80	0.03
Bio11 [a]	Mean temp of coldest quarter (°C)	0.78	0.54	−0.02
Bio12 [a]	Annual precipitation (mm)	0.83	−0.53	0.14
Bio13 [a]	precipitation of wettest month (mm)	0.86	−0.34	−0.11
Bio14 [a]	precipitation of driest month (mm)	0.75	0.42	0.49
Bio15	precipitation seasonality (mm)	−0.41	0.35	−0.73
Bio16 [a]	precipitation of wettest quarter (mm)	0.82	−0.47	−0.17
Bio17	precipitation of driest quarter (mm)	0.75	−0.42	0.51
Bio18 [a]	precipitation of warmest quarter (mm)	0.84	−0.46	−0.07
Bio19	precipitation of coldest quarter (mm)	0.75	−0.42	0.51
% Explained variance		45.1	29.4	13.1

[a] Most relevant variables according to histograms analysis.

2.2.2. *D. armandi* Distribution Data and Geographic Layer

The distribution data for *D. armandi* were obtained from relevant literature and field observations records of the Department of Forestry Protection. Table 4 illustrates the results of the records. In addition, we collected records via field investigation of *D. aramndi* from May to September 2012–2018. Name, longitude, latitude, and altitude were recorded for each occurrence. We divided the provinces into the largest survey units and then used the county forestry departments as the smallest survey units according to the infected districts. The route of investigation is carried out in order from west to east in China. The distance between the survey points is generally not less than 30 km. The sorted data were saved in the required format of BIOCLIM, ENFA, and MaxEnt. However, due to some occurrences being hardly explored, these records within the allowable range of error represent a credible data of the geographical distribution of *D. armandi*. These records were georeferenced on 1:4,000,000 administrative division map of China that was downloaded from the National Basic Geographic Information System (http://www.ngcc.cn).

Table 4. Occurrence records of *D. armandi*.

Province	Title 2	Records (County & Forestry Bureau)
Shaanxi	74	Chang'an District, Huyi District, Zhouzhi, Zhashui, Zhen'an, Ningshan, Shiquan, Langao, Zhenping, Ziyang, Hanying, Foping, Liuba, Mian, Xixiang, Zhenba, Nanzheng, Ningqiang, Taibai, Feng, Mei, Ningxi Forestry Bureau, Ningdong Forestry Bureau, Changqing Forestry Bureau, Hanxi Forestry Bureau, Longcaoping Forestry Bureau, etc.
Gansu	21	Hui, Liangdang, Wen, Cheng, Kang, Xiaolongshan Forestry Experiment Bureau, etc.
Henan	26	Lingbao, Lushi, Luoning, Luanchuan, Songshan, Lushan, Nanzhao, Xixia, Xichuan, Neixiang, etc.
Sichuan	17	Chaotian District, Lizhou District, Wangcang, Jiange, Nanjiang, Tongjiang, Wanyuan City, etc.
Chongqing Municipality	12	Chengkou, Kaizhou District, Wuxi, Fengjie, Wushan, etc.
Hubei	16	Zhuxi, Zhushan, Yunxi, Baokang, Badong, Shennongjia Nature Reserve, etc.

2.2.3. *P. armandi* Distribution Data

The Global Biodiversity Information Facility (GBIF) was used to gather information on *P. armandi* distribution. The GBIF contained 1088 records for *P. armandi*; only 646 records are from China. However, some records only differed minimally in their geographic coordinates and several contained incomplete data. Thus, 410 records were eliminated. In addition, *P. armandi* distribution data were also collected from records of each province's forestry bureau. The final known distribution of *P. armandi* included 236 records. Subsequently, the potential distribution of *P. aramndi* used MaxEnt was added into the analysis as a variable.

2.3. Bioclimatic Profile of *D. armandi*

A raw data of 167 records was gathered to identify the terrain preference of *D. armandi*, where it was most frequently found and the host preference that *D. armandi* attack with the highest frequency. The frequency of its incidence (IP) on different hosts was used as a measure standard with the degree of occurrence [33]. Before the potential distribution of *D. armandi* using SDMs, 48 records with minimally differences in geographic coordinates and elevation were discarded from data. Therefore, 119 presence-only records were composed *D. armandi* distribution data.

A bioclimatic profile of *D. armandi* was obtained from BIOCLIM in the DIVA-GIS v.7.5 (http://www.diva-gis.org/) (Table 5). The profile describes the habitat conditions where *D. armandi* has been found. Meanwhile, it is used to identify other locations where *D. armandi* may inhabit. The mean,

standard deviation, and minimum and maximum tolerance were applied to characterize the suitability limits of this beetle.

Table 5. Bioclimatic profile of *D. armandi* for each location (obtained using BIOCLIM).

Environmental Variables	Min.	Max.	Mean	SD	5%	10%	50%	90%	95%
Annual mean temp (°C)	5.6	17.1	11.6	2.7	7	7.5	12	15	15.3
Mean diurnal range (°C)	7	12	9.2	0.9	8	8	9	10	11
Isothermality	24	32	29.8	1.6	27	28	30	31	32
Temperature seasonality	718	970	792.8	55.6	728.9	735.8	782	885	902.3
Maximum temp of warmest month (°C)	21	33	26.4	3.1	22	22	26	31	32
Minimum temp of coldest month (°C)	−11	2	−4.6	2.8	−10	−9	−4	−1	−1
Temperature annual range	28	38	31	2.3	29	29	30	34	36
Mean temp of wettest quarter (°C)	14	26	20.3	3.0	16	16	20	24	25
Mean temp of driest quarter (°C)	−5	7	1.5	2.7	−3.1	−2.2	2	4	5
Mean temp of warmest quarter (°C)	15	27	21.2	3.1	16	17	21	25	26
Mean temp of coldest quarter (°C)	−5	7	1.5	2.7	−3.1	−2.2	2	4	5
Annual precipitation (mm)	579	1286	910	181.9	671.8	695.8	878	1195.2	1248.8
precipitation of wettest month (mm)	118	232	165.8	28.1	127.9	132	159	204.4	211
precipitation of driest month (mm)	3	22	9.6	4.7	4	4	8	17	19
precipitation seasonality (mm)	63	94	72.2	6.7	64	65	72	81	83
precipitation of wettest quarter (mm)	301	564	436.2	66	348	362.8	423	524	544.6
precipitation of driest quarter (mm)	12	74	35.3	15.8	15	17	31	59	67
precipitation of warmest quarter (mm)	269	552	405.6	73.7	317.9	323	381	510	535.7
precipitation of coldest quarter (mm)	12	74	35.3	15.8	15	17	31	59	67
Altitude (m a.s.l.)	1323.5	2333.9	1815.9	213.9	1490	1559	1807	2114	2200

2.4. Current Potential Distribution (SDMs)

2.4.1. Potential Distribution of *D. armandi* Using BIOCLIM

D. armandi distribution data and the screened bioclimatic variables were imported into DIVA-GIS v.7.5 (http://www.diva-gis.org/), where all of the data were processed and analyzed using BIOCLIM. The potential distribution map of *D. armandi* was obtained from layer processing in ArcGIS v.10.2. The possibility was divided into four categories: null (Occurrence Probability = 0), low (0 < Occurrence Probability ≤ 2.5 percentile), moderate (2.5 < Occurrence Probability ≤ 7 percentile), and high (7 < Occurrence Probability ≤ 100 percentile).

The model was trained and validated using cross-validation. The *D. armandi* distribution points were randomly divided into two subsets. The model was trained using 75% of the data, and the remaining data were independently evaluated. The model was evaluated using the area under the receiver operating characteristic curve (AUC), Kappa, and the True Skills Statistic (TSS) [34]. The AUC is a threshold independent measure of accuracy that compares the rate of true and false positives of validation data across all of the available habitat suitability thresholds, where values that are close to 1 indicate perfect discrimination capacity, values close to 0 indicate poor discrimination capacity, and values close to 0.5 indicate discrimination capacity no greater than random [35]. We generated 100 pseudo absence points using ArcMap by randomly generating points [36].

2.4.2. Potential Distribution of *D. armandi* Using ENFA

All of the layers were transformed into Idrisi Grid format, and subsequent analyses were conducted while using the ENFA algorithm available in BioMapper v.4.0 (http://www.unil.ch/biomapper). The relationship between the EGVs was determined, and the combination of the variables tested was established and then transformed into two types of uncorrelated factors with equal numbers, forming a multidimensional environmental gradient space for calculating habitat suitability. Thus, the screened variables and the distribution of *P. armandi* were both added to the analysis.

The marginality and the specialization can characterize the habitat suitability (HS). The marginality (M) is defined as the absolute difference between the global mean (average value of the global distribution, m_G) and the mean of the species (m_S), divided by 1.96 standard deviations (σ_G) the global distribution. The specialization (S) is defined as the ratio of the standard deviation of global

distribution and the standard deviation of the studied species [37]. The HS grades were divided into four ranks: null (0–10), low (11–30), moderate (31–60), and high (61–100).

The robustness of the model was evaluated in BioMapper v.4.0 (http://www.unil.ch/biomapper) by using k-fold jackknife-type cross-validation. The *D. armandi* distribution points were randomly divided into k (k = 4) parts. The model was calibrated by using the k-1 part, and the remaining parts were validated. After k repetitions, the model was judged while using the Boyce's continuous index. The grading threshold of HS is determined based on the relationship between the observed and the expected values [38]. The closer the value of the index is to 1, the higher the accuracy of the model being evaluated.

2.4.3. Potential Distribution of *D. armandi* Using MaxEnt

All of the layers were converted to raster format via ArcTools in Arc-GIS v.10.2 (Environmental System Research Institute Inc., Redlands, CA, USA). Subsequently, the screened variables and the distribution of *P. armandi* were analyzed while using MaxEnt. Eventually, the potential distribution of *D. armandi* was obtained by using the "extraction analysis" function in Arc-GIS v.10.2. During model running, 75% of the points were used for model training, whereas the remaining points were used for the model test. The output format was in a logistic format, and the remaining parameters selected the default value of the model. The probability (0–1) of species presence was displayed on the distribution map and the probability values were divided into four grades: null (0–0.1), low (0.11–0.3), moderate (0.31–0.6), and high (0.61–1). The model accuracy was assessed using AUC, Kappa, and the TSS.

3. Results

3.1. Bioclimatic Profile of *D. armandi*

The preferential altitudinal range for *D. armandi* varied between 1300 m a.s.l and 2350 m a.s.l. The slope ranges were mostly from 25° to 35°, and the southern aspect obviously occupied a large proportion (Figure 2). The percentage of incidence showed 98.21% frequency attacks by this beetle on *P. armandi* (Table 6).

Table 6. Incidence (%) of *D. armandi* in China.

Pinus Species	Incidence (%)
P. armandi Franch	98.21
P. tabulaeformis Carr. (Pinaceae)	1.79
P. massoniana Lamb.	0
P. bungeana Zucc. ex Endl.	0
Larix principis-rupprechtii Mayr	0

Bioclimatic profile of *D. armandi* (Table 5) suggests that the areas where this beetle exists support the following temperatures: annual mean temperatures of 5.5–17 °C, mean diurnal range of 7–12 °C, temperature annual range of 28–38 °C, maximum temperature of warmest month range of 21–33 °C, minimum temperature of coldest month range of −11–2 °C, and mean temperatures of the driest quarter and mean temperatures of the coldest quarter being consistent, with −5–7 °C. In terms of precipitation, the habitats have the following characteristics: annual rainfalls of 579–1286 mm, wettest-month rainfalls of 118–232 mm, driest-month rainfalls of 3–22 mm, wettest-quarter rainfalls of 301–564 mm, and warmest-quarter rainfalls of 269–552 mm, and precipitation of driest quarter and precipitation of coldest quarter had the same result, 12–74 mm.

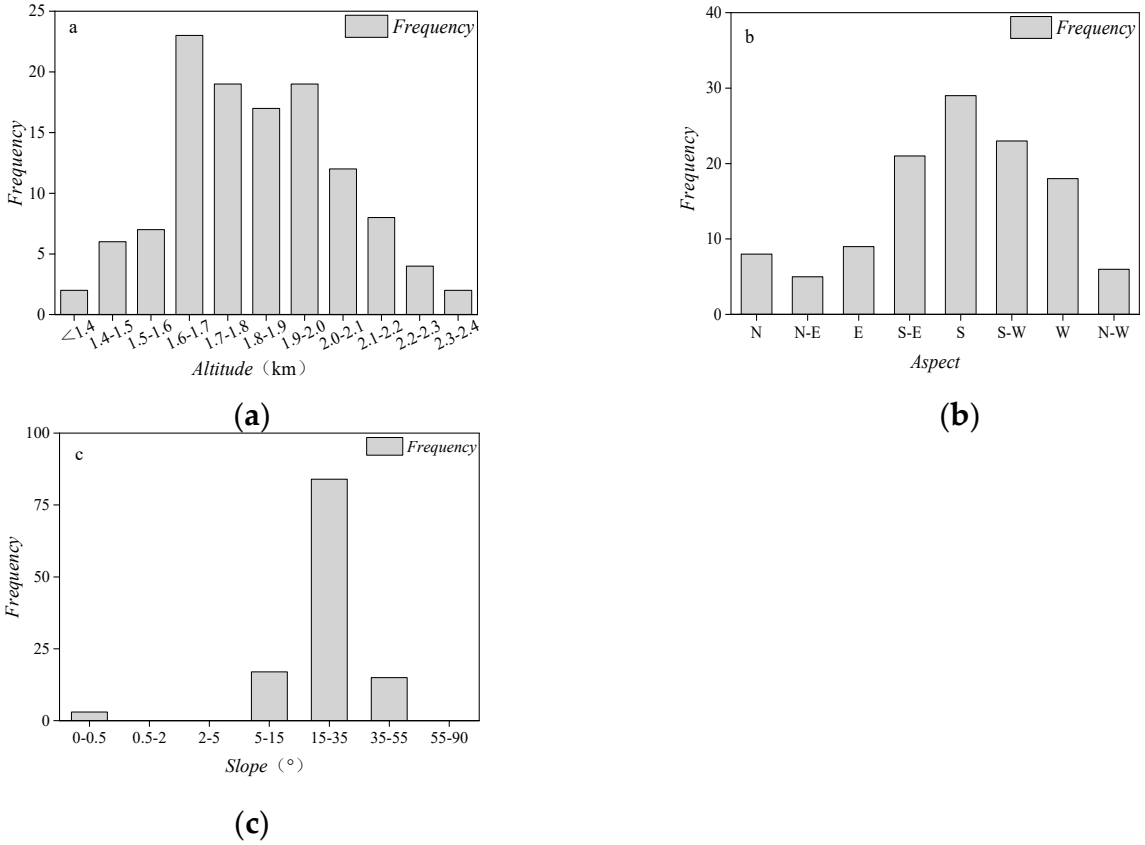

Figure 2. The frequency histogram of terrain variables. (**a**) altitude; (**b**) aspect. The aspect is measured counterclockwise in degrees, ranging from 0 degrees (true north) to 360 degrees (still true north, one cycle); and, (**c**) slope. According to the Geomorphological Survey and Geomorphologic Mapping Committee of the International Geographical Union, the grades of slopes are classified, as follows: 0°–0.5°for plains, 0.5°–2°for micro-slopes,2°–5° is a gentle slope,5°–15° is a slope, 15°–35°is a steep slope, 35°–55°is a steep slope, and 55°–90°is a vertical wall.

3.2. Variables Selection

Eight predictor bioclimatic variables were selected. Temperature variables Bio1, Bio6, Bio9, and Bio11 and precipitation variables Bio12, Bio13, Bio16, and Bio18. The responses of the bioclimate variables that influenced the potential geographical distribution of *D. armandi* are shown in response curves (Figure 3). These response curves show changes in the logistic prediction when each environmental variable changes by keeping all the other environment variables at their average value. In addition, altitude, aspect, slope, and the distribution of the host were also added in the analysis.

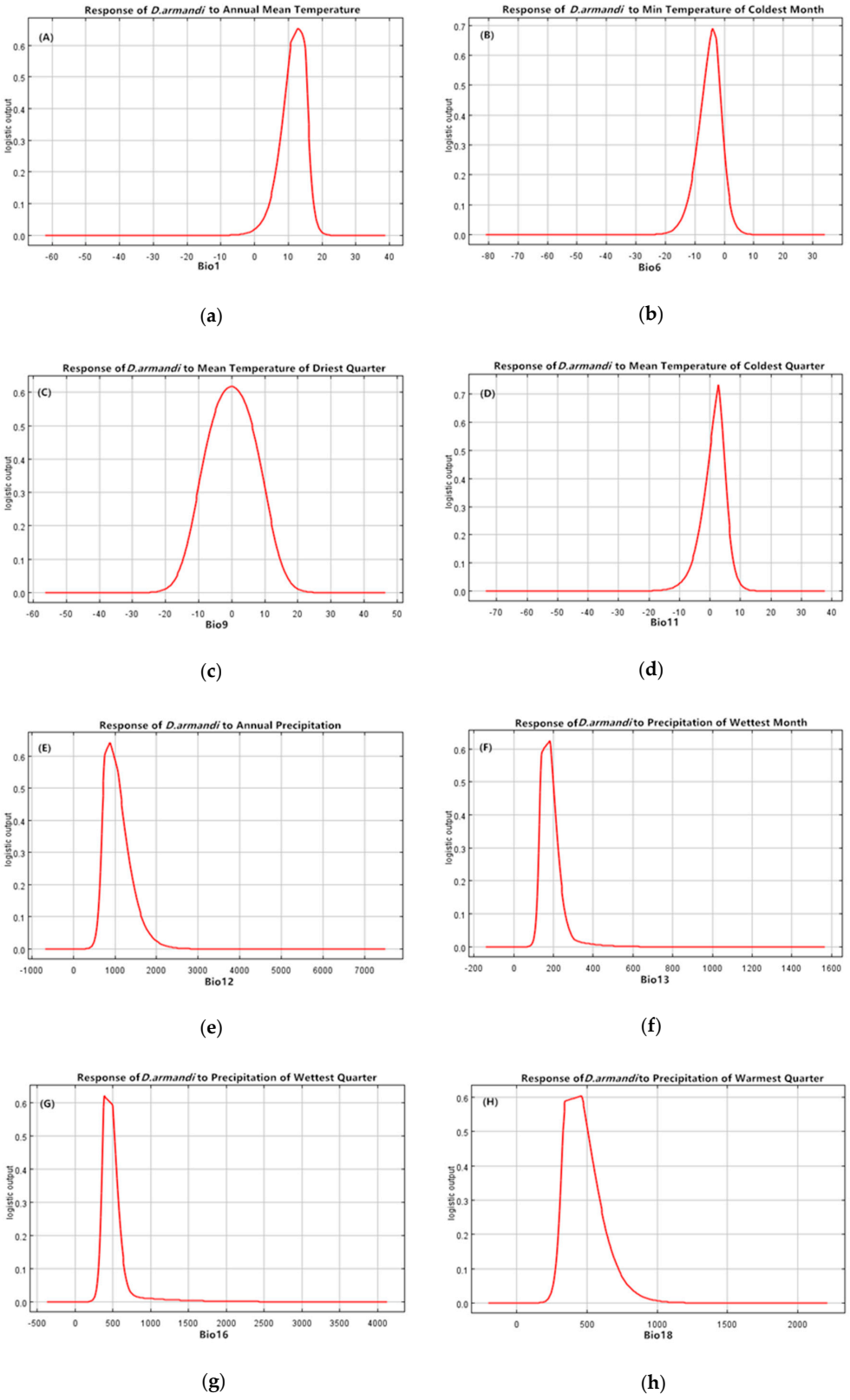

Figure 3. Response curves for the predictors of the MaxEnt Model.

3.3. Potential Distribution of *D. armandi* Using SDMs

The *D. armandi* distribution map that was generated using BIOCLIM showed a continuous and high suitable environment that involved six provinces, along the entire range of the Qinling Mountains

and the Ta-pa Mountains (Figure 4). Particularly, the high area showed a situation where the center radiated outward. The AUC value was 0.809, which reached the "good" standard, indicating that the results could be used to study the suitability division of *D. aramndi*. The Kappa was 0.505 and TSS was 0.523. The habitat suitability map showed that the potential distribution of *D. armandi* was focused on the Qinling Mountains and the Ta-pa Mountains (Figure 5). The high HS areas can be found along the entire the Qinling Mountains and the Ta-pa Mountains, scattering discontinuous patches scattered. The areas of moderate suitability are embedded in these plaques. It is worth noting that the model had better definition than BIOCLIM and the biological significance of the variables is clearer. The global marginality factor was 2.168, which suggests that the regions where *D. armandi* exist support climatic conditions that differ from the prevalent conditions in the Qinling Mountains and the Ta-pa Mountains. The global tolerance was 0.213 (tolerance = 1/specialization), which suggests that *D. armandi* has low tolerance to environmental changes, namely the ecological niche of this beetle is relatively narrow when it comes to some variables in the Qinling Mountains and the Ta-pa Mountains. The first four factors explained 91.6% of the total variation (Table 7). In terms of the marginality factor, the preference of *D. armandi* is closely related to the mean temperature of the coldest quarter (−0.377), mean temperature of driest quarter (−0.314), precipitation of wettest quarter (0.301), minimum temperature of coldest (−0.300), annual mean temperature (−0.269), precipitation of wettest month (0.234), annual precipitation (0.211), altitude (0.201), aspect (0.176), *P. armandi* distribution (0.171), and slope (0.153). The tolerance factors indicate that *D. armandi* is associated with annual precipitation (−0.309), mean temperature of coldest quarter (−0.210), mean temp of driest quarter (−0.206), and precipitation of wettest quarter (−0.157). Boyce's continuous index is 0.853, which indicated that the model is adequately robust. The potential distribution map that was obtained from MaxEnt displayed that *D. armandi* was concentrated in the Qinling Mountains and the Ta-pa Mountains (Figure 6). Almost all of the Qinling Mountains and the Ta-pa Mountains appear to be moderate and high suitability areas, which are geographically connected. The potential distribution for *D. armandi* obtained the results corresponding to the relative contributions of the variables that were employed for modeling, where the MaxEnt assigns the increase in gain to the environmental variables that are occupied, making a conversion to a percentage. The limited factors of potential distribution of *D. armandi* had a mean temperature of coldest quarter (29.1%), mean temperature of driest quarter (15.1%), minimum temp of coldest month (14.8%), altitude (12.6%), precipitation of wettest quarter (9.7%), annual mean temp (6.9%), and precipitation of warmest quarter (5.5%) (Table 8). AUC, Kappa, and TSS analyzed the model performance, which gave a very accurate result. The AUC was 0.934, Kappa was 0.560, and TSS was 0.595.

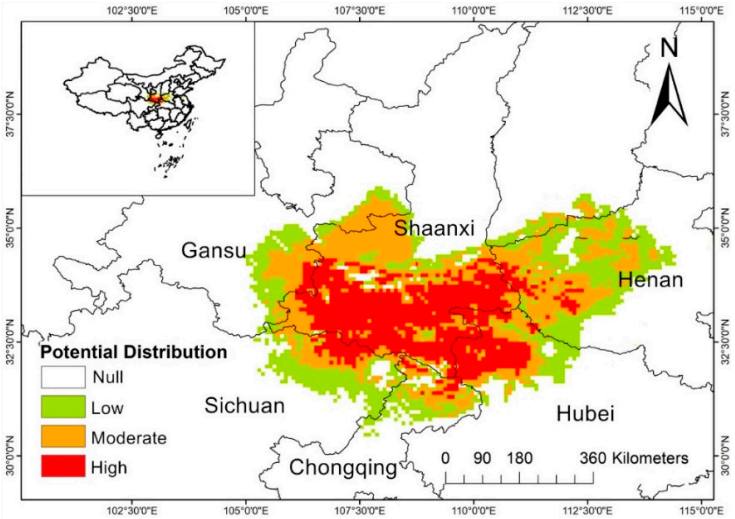

Figure 4. Potential distribution of *D. armandi* in China modeled with BIOCLIM.

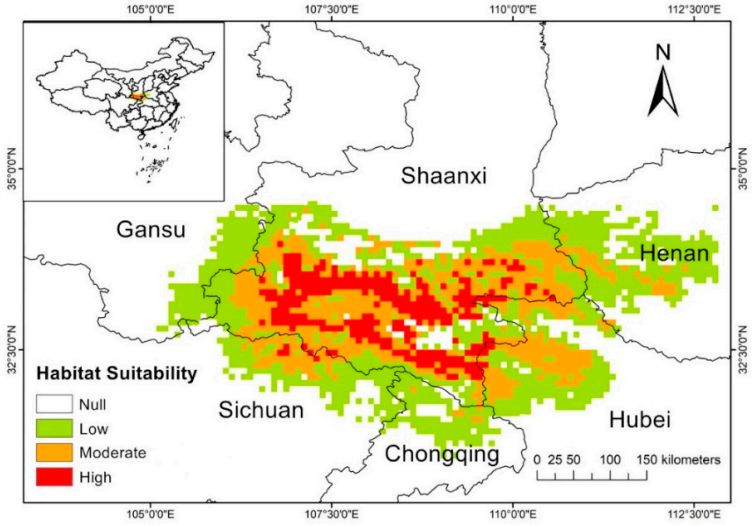

Figure 5. Habitat suitability (HS) for *D. armandi* in China modeled with ENFA.

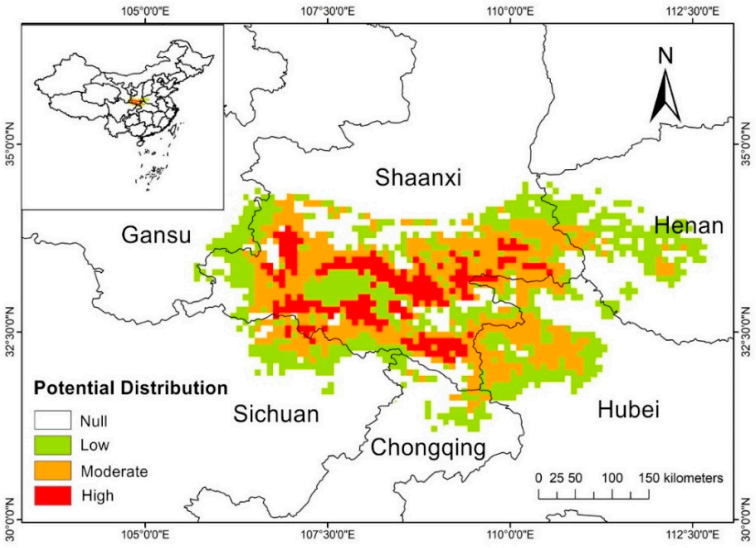

Figure 6. Potential distribution of *D. armandi* in China modeled with MaxEnt.

Table 7. The first four factors and coefficients of Ecogeographic Variables (EGVs) to factors generated by Ecological Niche Factor Analysis (ENFA).

Category	Ecogeographic Variable (EGVs)	*D. armandi*			
		MF (100%) SF1 (28%)	**SF2 (47.9%)**	**SF3 (9.4%)**	**SF4 (6.3%)**
Climate	Annual mean temp	−0.269 *	−0.018	−0.070	−0.011
	Minimum temp of coldest month	−0.300 *	0.027	0.015	0.000
	Mean temp of driest quarter	−0.314 *	0.084	0.206 *	0.043
	Mean temp of coldest quarter	−0.377 *	0.177 *	−0.200 *	−0.210 *
	Annual precipitation	0.211 *	0.101	−0.080	−0.309 *
	Precipitation of wettest month	0.234 *	0.011	0.004	0.000
	Precipitation of wettest quarter	0.301 *	0.036	0.157 *	0.004
	Precipitation of warmest quarter	0.133	0.032	0.079	0.023
Terrain	Altitude	0.201 *	0.001	0.001	0.000
	Aspect	0.176 *	0.000	0.001	0.000
	Slope	0.153 *	0.000	0.000	0.000
Host	*P. armandi* distribution	0.171 *	−0.036	−0.027	0.000

MF: marginality factors, SF: specialization factors. The EGVs marking the largest contribution (≤−0.15 or ≥0.15) to each factor are represented with asterisk. For the first factor, positive and negative signs indicate the preference by the species for values above and below the mean for each EGV, respectively. For the remaining factors, the signs have no ecological relevance.

Table 8. Percentage of estimated contribution for EGVs by using MaxEnt.

Ecogeographic Variables	% Contribution
Mean temp of coldest quarter	29.3
Mean temp of driest quarter	15.1
Minimum temp of coldest month	14.8
Altitude	12.6
Precipitation of wettest quarter	9.7
Annual mean temp	6.9
Precipitation of warmest quarter	5.5
Precipitation of wettest month	2.8
Annual precipitation	1.4
Aspect	1.1
Slope	0.8
Host distribution	0.1

4. Discussion

The potential geographical distribution of insects and the formation of infestations are closely related to the ecological environment [39]. SDMs can be employed to identify the bioclimatic profile of a species and determine the potential distribution while integrating occurrence data with environmental variables [13,40]. Therefore, the potential distribution of species can explain the species that exist in one area but not in another [41]. It is worth noting that, for specialist herbivorous insects, the distribution of the host is generally taken as the decisive factor that determines their range.

The results of this study showed that the potential geographical distribution of *D. armandi* was concentrated in the Qinling Mountains. In other words, *D. armandi* was limited to specific regions within the Qinling Mountains and the Ta-pa Mountains, despite hosts occurring in northern and southwestern China. Conversely, many studies suggest that host distribution at the macro-scale level determines the distribution of bark beetles. However, our results indicate that the distribution of *D. armandi* is limited by temperature and precipitation rather than the geographical distribution of *P. armandi*. For example, Carroll et al. (2004) [42] considered that the latitudinal and elevational range of mountain pine beetle, *Dendroctonus ponderosae*, is not limited by available hosts. Instead, it is limited by minimum temperature in western Canada. Accordingly, its potential to expand north and east has been restricted by climatic conditions that are unfavorable for brood development. Ma et al. (2011) [43] reported that the maximum temperature isotherms limit the geographical distribution of *Dendroctonus rhizophagus* in the Sierra Madre Occidental, Mexico. Ungerer et al. (1999) [44] deemed that the dispersal of *Dendroctonus frontalis* into more northerly areas of the United States was limited by the isotherm for minimum annual temperature. However, Bentz et al. (2010) [45] used the available population models and climate forecasts to explore the responses of *Dendroctonus rufipennis* and *Dendroctonus ponderosae* in western North America. The results suggested a movement of temperature suitability to higher latitudes and elevations that is based on projected warming. A 1.79% incidence by this beetle on *P. tabulaeformis* remains. In rare cases, it may also attack *P. tabulaeformis* [20]. Therefore, it is an important influencing factor for *D. armand*i, which *P. tabulaeformis* can be used as an alternative host in the future climate change.

The tolerance and marginality coefficients that were obtained from ENFA suggest that the ecological niche of *D. armandi* is relatively narrow when it comes to temperature and precipitation. Temperature is the most important climatic factor that affects two different aspects of insect biology that subsequently affect distribution: flight and larval development. However, it is important to note that temperature or other climatic factors may have different effects during different population phases of bark beetles [46]. The cold tolerance that is possessed by insects is a key factor in their adapting to the geographical environment. *D. armandi* overwinters primarily as larvae, and some pupae and adults also overwinter. Overwintering larvae begin pupate in early April and peak in the peak in May. The adults begin to fly in mid-April and reach the peak in mid-June. The spawning period begins in late April,

and in July, the first generation of adults begins to fly out, and some larvae directly enter the wintering stage [47]. Larval mortality is strongly temperature dependent, with winter being the most critical time [48]. The survival rate of an insect population at low temperatures in winter is directly related to its reproductive success [49]. The ENFA and the MaxEnt suggested that the mean temperature of coldest quarter/driest quarter played a considerable role in limiting the distribution of *D. armandi*. Wang et al. indicated that the supercooling point of *D. armandi* larvae reached −7.49 ± 0.21 °C in the coldest quarter [50]. However, the average temperature that northern China can attain is −10 °C, which far exceeds the average temperature of the coldest quarter (−5 °C) in the *D. armandi* occurrence zone. However, the precipitation of wettest quarter could be the main factor limiting the distribution of *D. armandi* in the Yunnan–Guizhou Plateau of southwest China. Precipitation changes the humidity of the environment, which in turn affects insect flight and reproduction [51]. The intermittent precipitation of the wettest quarter not only delayed *D. armandi* development time, but it also caused the death of *D. armandi* larvae. In addition, the flight diffusion activity for *D. armandi* was closely related to temperature [52]. The peak of the flight spread of *D. armandi* was concentrated during 14:00–16:30. The distribution of *D. armandi* on the trunk is firstly concentrated on the south and west, because the illumination time in the south and west of host trees is much longer than in the north and east. The climatic conditions where this beetle inhabit are different from the prevalent climate in the Qinling Mountains and the Ta-pa Mountains. In fact, the actual occurrences of this beetle in the unique climate of the Qinling Mountains and the Ta-pa Mountains also adequately explain that *D. armandi* would not advance into the northern and southwestern China at present.

In terms of terrain, the landscape where has interactions between the meso-scale atmospheric currents and the terrain can play an important role in governing the spread and impact of the dispersal capabilities for herbivores insect in forest ecosystems [53,54]. The influence of elevation on the distribution of *D. armandi* is not clear. However, the results from ENFA and MaxEnt both suggest that this factor is important. The temperature likely affects the altitudinal distribution of *D. armandi*. In addition, the preference elevation range of *D. armandi* is correlated with the dominant altitudinal distribution of *P. armandi*. The results of our study suggest that the preference of selection for slope and other aspects of the dispersal of *D. armandi* were important. The dominant terrain features in the region included valleys and canyons, which were shaped similar to a "U" or a "V". The majority of *D. armandi* infestations were found on the southern slope, in valleys and canyons, where the topography could act as a conduit for further dispersal. At those locations, dispersing *D. armandi* may behave like inert particles, causing terrain-induced tropospheric convective and advective currents that influence population dispersal and establishment [55]. Thus, there was a significant difference in the extent of tree mortality that was attributed to *D. armandi* between the southern and northern slopes. There are at least two reasons to explain the tendency of *D. armandi* to invade a region. On one hand, the hosts may be more susceptible on drier and sun-exposed south slopes. [56]. The effects of drought on herbivorous insect outbreaks in the U.S. suggested a non-linear relationship between drought intensity and outbreaks of aggressive bark beetle species (i.e., those that are capable of causing extensive levels of tree mortality), where moderate droughts reduce bark beetle population performance and subsequent tree mortality, whereas intense droughts, which frequently occur in the western U.S., increase bark beetle performance and tree mortality [57]. On the other hand, insects established on southern slopes may enjoy higher reproductive rates due to higher ambient temperatures than insects on shaded slopes [58].

The potential distributions of *D. armandi* not only clarify the factors influencing its distribution, but also can be used to prioritize treatments for potential management in the future. When considering that it plays an important role in the meso- and micro-levels, we should explore the variables, such as temperature, humidity, and topography, which directly affect the development of the life cycle and population dynamics of this bark beetle. For example, the changes of habitats of *D. armandi* under climate change conditions and predicting the potential spread of new infestations based on landscape

features in concert with new landscape scale spread modeling approaches, and so on, may need to be further studied.

5. Conclusions

In this study, we used SDMs to clarify the potential distribution of *D. armandi* in China and identify the factors influencing its distribution. We found that *D. armandi* almost exclusively attacked *P. armandi* and the distribution of *D. armandi* is plaque-like along the Qinling Mountains and the Ta-pa Mountains. The ecological niche of *D. armandi* is relatively narrow when it comes to these environmental variables, such as temperature and precipitation. *D. armandi* also has a narrow ecological niche with respect to the host distribution. The factors limiting the distribution of *D. armandi* include the mean temperature of the coldest quarter and precipitation of the wettest quarter. The mean temperature of the coldest quarter does not guarantee that *D. armandi* larvae can overwinter in northern China, and the precipitation of the wettest quarter plays an important role in the dispersal and colonization of *D. armandi* adults in southwestern China. With respect to the host, the distribution of *P. armandi* is not a limiting factor in the distribution of *D. armandi*. In regards to terrain variables, they create habitat selection preferences for *D. armandi*. *D. armandi* predominately colonizes trees on the southern slopes of valleys and canyons with elevations between 1300 m a.s.l and 2400 m a.s.l.

Author Contributions: Conceived and designed the experiments: H.N., H.C. Performed the experiments: H.N., D.F., B.L., H.W. Analyzed the data: H.N., L.D. Contributed reagents/materials/analysis tools: H.N. Wrote the paper: H.N.

Funding: This research was funded by the Natural Science Basic Research Plan in Shaanxi Province of China and the National Natural Science Foundation of China, grant number 2017ZDJC-03 and 31870636, respectively.

Acknowledgments: We acknowledge support with respect to a collection of insects from Huangguan Forest Farm of Ningxi Forestry Bureau, Shaanxi, China.

Conflicts of Interest: The authors declare no conflict of interest.

References

1. Shaver, G.R. Spatial Heterogeneity: Past, Present, and Future. In *Ecosystem Function in Heterogeneous Landscape*; Lovett, G.M., Jones, C.G., Eds.; Springer: New York, NY, USA, 2005; pp. 443–449.
2. Vinatier, F.; Tixier, P.; Duyck, P.F.; Lescourret, F. Factors and mechanisms explaining spatial heterogeneity: A review of methods for insect populations. *Methods Ecol. Evol.* **2011**, *2*, 11–22. [CrossRef]
3. Brown, J.H. On the relationship between abundance and distribution of species. *Am. Nat.* **1984**, *124*, 255–279. [CrossRef]
4. Thomas, C.D.; Bodsworth, E.J.; Wilson, R.J.; Simmons, A.D.; Davies, Z.G. Ecological and evolutionary processes at expanding range margins. *Nature* **2001**, *411*, 577–581. [CrossRef]
5. Buckley, H.L.; Hannah, L.; Freckleton, R.P. Understanding the role of species dynamics in abundance-occupancy relationships. *J. Ecol.* **2010**, *98*, 645–658. [CrossRef]
6. MacDonald, G.M. Biogeography: Introduction to Space, Time and Life. *Prof. Geogr.* **2010**, *55*, 283–285.
7. Rodríguez, J.; Brotons, L.; Bustamante, J.; Seoane, J. The application of predictive modeling of species distribution to biodiversity conservation. *Divers. Distrib.* **2007**, *13*, 243–251. [CrossRef]
8. Kearney, M.; Porter, W. Mechanistic niche modelling: combining physiological and spatial data to predict species' ranges. *Ecol. Lett.* **2009**, *12*, 334–350. [CrossRef]
9. Matern, A.; Drees, C.; Kleinwächter, M.; Assmann, T. Habitat modelling for the conservation of the rare ground beetle species *Carabus variolosus* (Coleoptera, Carabidae) in the riparian zones of headwaters. *Biol. Conserv.* **2007**, *136*, 618–627. [CrossRef]
10. Srivastava, V.; Griess, V.C.; Padalia, H. Mapping invasion potential using ensemble modelling. A case study on Yushania maling in the Darjeeling Himalayas. *Ecol. Modell.* **2018**, *385*, 35–44.
11. Miller, J. Species distribution modeling. In *Geography Compass*; Mike, B., Ed.; Wiley: Hoboken, NJ, USA, 2010; pp. 490–509.
12. Pearson, R.G.; Dawson, T. Predicting the impacts of climate change on the distribution of species: Are bioclimate envelope models useful? *Glob. Ecol. Biogeogr.* **2003**, *12*, 361–371. [CrossRef]

13. Beaumont, L.J.; Hughes, L.; Poulsen, M. Predicting species distributions: use of climatic parameters in BIOCLIM and its impact on predictions of species' current and future distributions. *Ecol. Model.* **2005**, *186*, 251–270. [CrossRef]
14. Elith, J.; Franklin, J. Species Distribution Modeling. In *Encyclopedia of Biodiversity (Second Edition)*; Simon, A.L., Ed.; Academic Press: Waltham, MA, USA, 2013; pp. 692–705.
15. Booth, T.H. Why understanding the pioneering and continuing contributions of BIOCLIM to species distribution modelling is important. *J. Austral. Ecol.* **2018**, *43*, 852–860. [CrossRef]
16. Giusti, M.; Bo, M.; Angiolillo, M.; Cannas, R.; Cau, A. Habitat preference of *Viminella flagellum* (Alcyonacea: Ellisellidae) in relation to bathymetric variables in southeastern Sardinian waters. *Cont. Shelf Res.* **2017**, *138*, 41–45. [CrossRef]
17. Palfreyman, J.; Graham-Brown, J.; Caminade, C.; Gilmore, P.; Otranto, D. Predicting the distribution of Phortica variegata and potential for *Thelazia callipaeda* transmission in Europe and the United Kingdom. *Parasit Vectors* **2018**, *11*, 272. [CrossRef]
18. Van Gils, H.; Westinga, E.; Carafa, M.; Antonucci, A.; Ciaschetti, G. Where the bears roam in Majella National Park, Italy. *J. Nat. Conserv.* **2014**, *22*, 23–34. [CrossRef]
19. Huang, M.; Ge, X.; Shi, H.; Tong, Y.; Shi, J. Prediction of Current and Future Potential Distributions of the *Eucalyptus* Pest *Leptocybe invasa* (Hymenoptera: Eulophidae) in China Using the CLIMEX Model. *Pest Manag. Sci.* **2019**. [CrossRef] [PubMed]
20. Chen, H.; Tang, M. Spatial and Temporal Dynamics of Bark Beetles in Chinese White Pine in Qinling Mountains of Shaanxi Province, China. *Environ. Entomol.* **2007**, *36*, 1124–1130. [CrossRef] [PubMed]
21. Dai, L.; Ma, M.; Wang, C.; Shi, Q.; Zhang, R. Cytochrome P450s from the Chinese white pine beetle, *Dendroctonus armandi* (Curculionidae: Scolytinae): Expression profiles of different stages and responses to host allelochemicals. *Insect Biochem. Mol. Biol.* **2015**, *65*, 35–46. [CrossRef] [PubMed]
22. Wang, D.; Liu, J.; Li, D.; Lei, R.; Lan, G. Community characteristics of *Pinus armandi* forest on Qinling Mountains. *J. Appl. Ecol.* **2004**, *15*, 357–362.
23. Zhang, B.S. Geomorphology of the Qinling mountains. *J. Northwest. Univ.* **1981**, *1*, 81–87.
24. Duque-Lazo, J.; Navarro-Cerrillo, R. What to save, the host or the pest? The spatial distribution of xylophage insects within the Mediterranean oak woodlands of Southwestern Spain. *For. Ecol. Manag.* **2017**, *392*, 90–104.
25. Buse, J.; Schröder, B.; Assmann, T. Modelling habitat and spatial distribution of an endangered longhorn beetle–a case study for saproxylic insect conservation. *Biol. Conserv.* **2007**, *137*, 372–381. [CrossRef]
26. Lausch, A.; Fahse, L.; Heurich, M. Factors affecting the spatio-temporal dispersion of *Ips typographus* (L.) in Bavarian Forest National Park: A long-term quantitative landscape-level analysis. *For. Ecol. Manag.* **2011**, *261*, 233–245.
27. Zhang, Y.; Cai, H. Geographical distribution and community ecological characteristics of *P. armandi*. *Hunan For. Sci. T.* **1989**, *4*, 5–8.
28. Zi, S.; Xiong, P.; Ma, L. Preliminary study on the prevention and control of the Chinese white pine beetle in Qinling Mountains and Ta-pa Mountains. *J. Green Sci. Technol.* **2016**, *5*, 41–42.
29. Cuellar, R.G.; Equihua, M.A.; Estrada, V.E.; Mendez, M.T.; Villa, C. Fluctuacion poblacional de *Dendroctonus mexicanus* Hopkins (Coleoptera: Curculionidae: Scolytinae) atraidos a trampas en el noroeste de Mexico y correlation con variables climaticas. *Boletin del Museo de Entomologia de la Universidad del Valle* **2012**, *13*, 12–19.
30. Hijmans, R.J.; Cameron, S.E.; Parra, J.L. Very high resolution interpolated climate surfaces for global land areas. *Int. J. Climatol.* **2005**, *25*, 1965–1978. [CrossRef]
31. Naimi, B.; Skidmore, A.K.; Groen, T.A.; Hamm, N.A. Spatial autocorrelation in predictors reduces the impact of positional uncertainty in occurrence data on species distribution modelling. *J. Biogeogr.* **2011**, *38*, 1497–1509. [CrossRef]
32. Graham, M.H. Confronting multicollinearity in ecological multiple regression. *Ecology* **2003**, *84*, 2809–2815. [CrossRef]
33. Salinas-Moreno, Y.; Ager, A.; Vargas, C.F.; Hayes, J.L.; Zúñiga, G. Determining the vulnerability of Mexican pine forests to bark beetles of the genus *Dendroctonus* Erichson (Coleoptera: Curculionidae: Scolytinae). *For. Ecol. Manag.* **2010**, *260*, 52–61. [CrossRef]
34. Allouche, O.; Tsoar, A.; Kadmon, R. Assessing the accuracy of species distribution models: prevalence, kappa and the true skill statistic (TSS). *J. Appl. Ecol.* **2006**, *43*, 1223–1232. [CrossRef]

35. Hanley, J.A.; McNeil, B.J. The meaning and use of the area under a receiver operating characteristic (ROC) curve. *Radiology* **1982**, *143*, 29–36. [CrossRef]
36. Jiménez-Valverde, A. Insights into the area under the receiver operating characteristic curve (AUC) as a discrimination measure in species distribution modelling. *Glob. Ecol. Biogeogr.* **2012**, *21*, 498–507. [CrossRef]
37. Hirzel, A.H.; Hausser, J.; Chessel, D.; Perrin, N. Ecological-Niche Factor Analysis: How to Compute Habitat-Suitability Maps without Absence Data? *Ecology* **2002**, *83*, 2027–2036. [CrossRef]
38. Hirzel, A.H.; Lay, G.L.; Helfer, V.; Randin, C.; Guisan, A. Evaluating the ability of habitat suitability models to predict species presences. *Ecol. Model.* **2006**, *199*, 142–152. [CrossRef]
39. Hortal, J.; Roura-Pascual, N.; Sanders, N.J.; Rahbek, C. Understanding (insect) species distributions across spatial scales. *Ecography* **2010**, *33*, 51–53. [CrossRef]
40. Anderson, R.P.; Lew, D.; Peterson, A.T. Evaluating predictive models of species' distributions: criteria for selecting optimal models. *Ecol. Model.* **2003**, *162*, 211–232. [CrossRef]
41. Lindenmayer, D.B.; Nix, H.A.; Mcmahon, J.P.; Hutchinson, M.F.; Tanton, M.T. The Conservation of Leadbeater's Possum, *Gymnobelideus leadbeateri* (McCoy): A Case Study of the Use of Bioclimatic Modelling. *J. Biogeogr.* **1991**, *18*, 371–383. [CrossRef]
42. Carroll, A.L.; Taylor, S.W.; Régnière, J.; Safranyik, L. Effect of climate change on range expansion by the mountain pine beetle in British Columbia. In *Mountain Pine Beetle Symposium: Challenges and Solutions*; Shore, T.L., Brooks, J.E., Eds.; Infromation Report BC-X.-399; Natural Resources Canada: Victoria, BC, Canada, 2003; p. 298.
43. Mendoza, M.G.; Salinas-Moreno, Y.; Olivo-Martínez, A.; Zúñiga, G. Factors influencing the geographical distribution of *Dendroctonus rhizophagus* (Coleoptera: Curculionidae: Scolytinae) in the Sierra Madre Occidental, Mexico. *Environ. Entomol.* **2011**, *40*, 549–559. [CrossRef]
44. Ungerer, M.J.; Ayres, M.P.; Lombardero, M.J. Climate and the northern distribution limits of *Dendroctonus frontalis* Zimmermann (Coleoptera: Scolytidae). *J. Biogeogr.* **1999**, *26*, 1133–1145. [CrossRef]
45. Bentz, B.J.; Régnière, J.; Fettig, C.J.; Hansen, E.M.; Hayes, J.L. Climate change and bark beetles of the western United States and Canada: direct and indirect effects. *BioScience* **2010**, *60*, 602–613. [CrossRef]
46. Økland, B.; Berryman, A. Resource dynamic plays a key role in regional fluctuations of the spruce bark beetles Ips typographus. *Agric. For. Entomol.* **2004**, *6*, 141–146. [CrossRef]
47. Wang, X.; Zhang, Z.; Yang, W. Preliminary study on the biological characteristics of *Dendroctonus armandi* (Coleoptera: Curculionidae: Scolytinae). *Sichuan For. Sci. Technol.* **2014**, *35*, 56–58.
48. Wang, J.; Gao, G.; Zhang, R.; Dai, L.; Chen, H. Metabolism and cold tolerance of Chinese white pine beetle *Dendroctonus armandi* (Coleoptera: Curculionidae: Scolytinae) during the overwintering period. *Agric. For. Entomol.* **2017**, *19*, 10–22. [CrossRef]
49. Bale, J.S.; Masters, G.J.; Hodkinson, I.D.; Awmack, C.; Bezemer, T.M. Herbivory in global climate change research: direct effects of rising temperature on insect herbivores. *Glob. Chang. Biol.* **2002**, *8*, 1–16. [CrossRef]
50. Wang, J.; Zhang, R.R.; Gao, G.Q.; Ma, M.Y.; Chen, H. Cold tolerance and silencing of three cold-tolerance genes of overwintering Chinese white pine larvae. *Sci. Rep.* **2016**, *6*, 34698. [CrossRef]
51. Jaworski, T.; Hilszczański, J. The effect of temperature and humidity changes on insects development their impact on forest ecosystems in the expected climate change. *For. Res. Pap.* **2013**, *74*, 345–355. [CrossRef]
52. Wang, X.L.; Chen, H.; Ma, C.; Li, Z. Chinese white pine beetle, *Dendroctonus armandi* (Coleoptera: Scolytinae), population density and dispersal estimated by mark-release-recapture in Qinling Mountains, Shaanxi, China. *Appl. Entomol. Zool. (Jpn.)* **2010**, *45*, 557–567. [CrossRef]
53. Bjornstad, O.N.; Mikko, P.; Liebhold, A.M.; Werner, B. Waves of larch budmoth outbreaks in the European Alps. *Science* **2002**, *298*, 1020–1023. [CrossRef] [PubMed]
54. Ims, R.A.; Leinaas, H.P.; Coulson, S. Spatial and temporal variation in patch occupancy and population density in a model system of an arctic Collembola species assemblage. *Oikos* **2010**, *105*, 89–100. [CrossRef]
55. Giroday, H.M.C.D.L.; Carroll, A.L.; Lindgren, B.S.; Aukema, B.H. Incoming! Association of landscape features with dispersing mountain pine beetle populations during a range expansion event in western Canada. *Landsc. Ecol.* **2011**, *26*, 1097–1110.
56. Powers, J.S.; Sollins, P.; Harmon, M.E.; Jones, J.A. Plant-pest interactions in time and space: A Douglas-fir bark beetle outbreak as a case study. *Landsc. Ecol.* **1999**, *14*, 105–120. [CrossRef]

57. Kolb, T.E.; Fettig, C.J.; Ayres, M.P.; Bentz, B.J.; Hicke, J.A. Observed and anticipated impacts of drought on forest insects and diseases in the United States. *For. Ecol. Manag.* **2016**, *380*, 321–334. [CrossRef]
58. Mattson, W.J.; Haack, R.A. The role of drought in outbreaks of plant-eating insects. *BioScience* **1987**, *37*, 110–118. [CrossRef]